AUTOMATIC METHANE PLUME QUANTIFICATION USING SENTINEL-2 TIME SERIES

T. Ehret[1] *A. De Truchis*[2] *M. Mazzolini*[2] *J.-M. Morel*[1] *G. Facciolo*[1]

[1]Université Paris-Saclay, CNRS, ENS Paris-Saclay, Centre Borelli, France
[2]Kayrros SAS

ABSTRACT

Methane emissions monitoring is essential to control methane pollution. In this paper, we propose an automatic practical methodology using time series to estimate the quantity of methane in a given plume using a multispectral satellite like Sentinel-2. Sentinel-2 proposes a low revisit time, a good spatial resolution and a low acquisition cost. Contrary to previous methods, the proposed approach does not require a manual selection of an optimal reference image. We compared its performance on an oil-and-gas site in Kazakhstan. This is the first step toward an automatic global monitoring system for methane plume detection and quantification with these satellites.

***Index Terms*—** Methane, quantification, automatic, monitoring, satellite, sentinel-2

1. INTRODUCTION

Recently, the detection of large and frequent methane emissions has raised concerns in the ability of natural gas to effectively reduce greenhouse gas emissions as a substitute to coal [1, 2]. Over a 20-year horizon, a methane molecule has a global warming potential about 85 times larger than carbon dioxide [3]. However, it has also been shown that a large part of methane emissions could be controlled or avoided [4]. This show that methane monitoring is now essential to reduce methane pollution.

Airborne campaigns [5] are often used to perform monitoring. While these campaigns have very good spatial resolutions and low detection thresholds, they suffer from a limited spatial coverage. Indeed, these campaigns can only cover a limited area and are costly to perform so they often have very limited revisit.

In order to perform a more global monitoring of greenhouse gas emissions produced by human activities, several satellites, such as GOSAT and TROPOMI [6], have been placed in orbit over the past ten years. Contrary to airborne campaigns, these satellites cover the entire Earth daily and were used successfully to detect unintended very large emissions [7]. However, it is difficult to detect small emissions due to its very low spatial resolution (5-7km). An alternative would be high resolution hyperspectral satellites such as PRISMA [8] and GHGSat [9]. However, the tasking nature, the relatively small field of view and the cost of data makes them unsuitable for a recurrent global monitoring.

The Sentinel-2 mission presents many advantages: it is recurrent with a low revisit time, it covers the entire planet and has a low acquisition cost. Sentinel-2 images comprise 12 bands, from visible to SWIR, with spatial resolutions from 10m per pixel to 60m per pixel. Although it was not initially designed for methane detection, it has been shown by Varon *et al*. [10] that some the bands are sensitive enough to methane to allow detection of moderate CH_4 emissions.

In this work, we propose an automatic methodology to quantify methane plumes using a multi-spectral satellites such as Sentinel-2 or Landsat-8. Starting from a timeseries of Sentinel-2 images, the background image without any methane plume is estimated by doing a temporal regression. The quantity of methane corresponding to the plume is then estimated for each pixel using an approximated atmospheric model.

2. AUTOMATIC METHANE QUANTIFICATION FROM MULTI-SPECTRAL TIME SERIES

We focus on the quantification of isolated excess concentrations of methane in the atmosphere. As shown in Fig. 1, bands B11 and B12 of Sentinel-2A are impacted by the presence of methane in the atmosphere. This means that it is possible to detect the presence of methane based on the dimming caused by the concentration of the gas.

The Beer-Lambert law states that for a light source with intensity I_0 and a wavelength λ

$$I = I_0 e^{-\sum_{i=0}^{N} A_i(\lambda) l_i}, \tag{1}$$

where the light goes through N gases defined by their absorption $A_i(\lambda)$ and equivalent optical path length l_i defined as the product of the actual optical path and the concentration of the i$^{\text{th}}$ gas. In our case, the light source is the sun and I_0 corresponds to its intensity in the SWIR spectrum. It is usually assumed that I_0 is constant. Taking into account that the

It was partly financed by Office of Naval research grant N00014-17-1-2552, DGA Astrid project « filmer la Terre » n° ANR-17-ASTR-0013-01, MENRT.

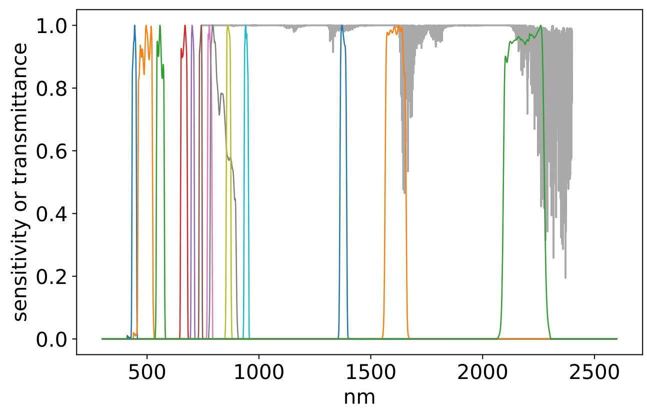

Fig. 1. Methane transmittance spectrum for 1cm of methane, in gray, and Sentinel-2A spectral sensitivity for all its bands, one color for each band. Bands B11 (1568-1659 nm, in orange on the right) and B12 (2114-2289 nm, in green on the right) are impacted by the presence of methane in the atmosphere thus allowing its measurement.

sensor of a satellite integrates over a band of wavelengths described by a sensitivity function s, the intensity of the light seen by a space-borne sensor becomes

$$I = I_0 \int s(\lambda)\alpha(\lambda)e^{-\gamma \sum_{i=0}^{N} A_i(\lambda)l_i} d\lambda, \tag{2}$$

where the two passes through the atmosphere are taken into account in γ, which is a function of both the sun azimuth angle θ_{sun} and the satellite view angle θ_{sat} (both defined in Fig. 2 such as $\gamma = \frac{1}{\cos(\theta_{sun})} + \frac{1}{\cos(\theta_{sat})}$). The albedo $\alpha(\lambda)$ models the reflection on the ground.

In practice, the atmosphere model can be well approximated with a simple fixed "pure methane atmosphere". This means that $N = 1$, l_{atm} the quantity of methane in the atmosphere is considered fixed and the only absorption coefficient is A_{CH4}. We discuss this approximation in Section 4. In the presence of a methane emission, characterized by l_{em}, the intensity of the light seen by the sensors then becomes

$$I_{em} = I_0 \int s(\lambda)\alpha(\lambda)e^{-\gamma A_{CH4}(\lambda)(l_{atm}+l_{em})} d\lambda. \tag{3}$$

The problem is that α is usually unknown. We propose to estimate its contribution by estimating the observation without methane, also called background observation, I_{bg}. When we assume that methane emissions are anomalous events, it is to be expected that most observations in a time series should not contain excess methane. So, if we suppose that α is rather stable in time, the time series can be used to estimate a methane free background model that can be compared with the current observation. Here, we compute the background for a given date as its linear regression over the previous dates. If we denote by I_t the observation at time t, then the

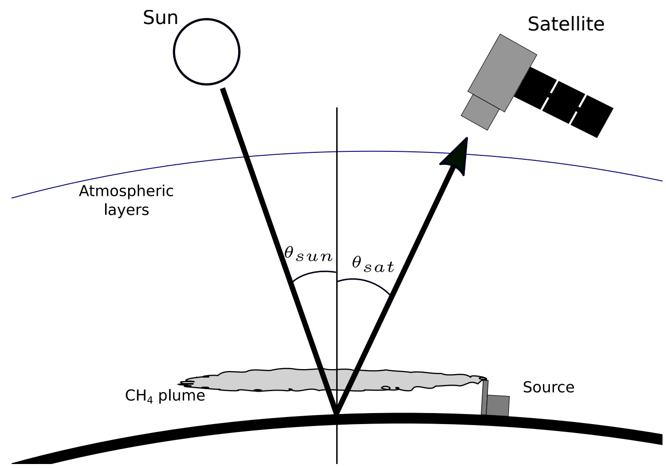

Fig. 2. Observation model for a satellite like Sentinel-2 with a passive sensor.

regression computes the optimal weights w_i that solve

$$\min_{\{w_i\}} \left\| I_t - \sum_{i=0}^{t-1} w_i I_i \right\|^2 . \tag{4}$$

Then the background is obtained as the linear combination $I_{bg} = \sum_{i=0}^{t-1} w_i I_i$. The estimation is performed on the logarithm of the images so as to limit the impact of abnormal high values in the SWIR bands. To further improve the background subtraction we combine this estimation with a band ratio that exploits the correlation between SWIR bands, similarly to the *multiple-band single-pass* (MBSP) from Varon *et al.* [10].

Since γ is known for each acquisition, this ratio only depends on the methane excess. Therefore, it is possible to estimate the value of l_{em} as the solution of a simple optimization problem

$$\arg\min_{l_{em}} \left\| \frac{I_{em}}{I_{bg}} - \frac{\int_{B12} s(\lambda)e^{-\gamma A_{CH4}(\lambda)(l_{em}+l_{atm})} d\lambda}{\int_{B12} s(\lambda)e^{-\gamma A_{CH4}(\lambda)l_{atm}} d\lambda} \right\|_2^2 . \tag{5}$$

This quantification scheme can also be adapted when using band ratio.

3. EXPERIMENTS

We consider an area of interest of size approximately 5x5 km^2 in Kazakhstan located on an oil-and-gas location. The size of this area is large enough so that the background estimation is not impacted too much by the presence of methane in the input images. We collected the L1C Sentinel-2 time series corresponding to this location and, using a cloud detection algorithm such as the one proposed by Dagobert *et al.* [11], we removed all images with a cloud coverage of more than 15% of the image pixels. We then manually detected the plume shown in this section.

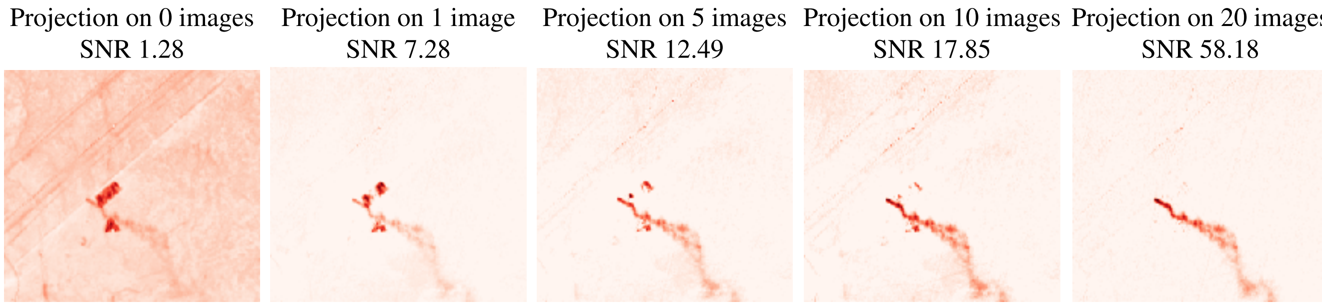

Fig. 3. Impact of the number of images used during the background estimation. A longer time series improves the SNR of the extracted plume in the residual thus helps its quantification. The SNR was estimated using a plume mask that was manually annotated.

We compared the quality of the reconstruction using a different amount of images for the background estimation. From Fig. 3, we can see that using a longer time series allows for a better background reconstruction. Indeed, after subtraction of the estimated background, the plume becomes much more visible and therefore its signal-to-noise ratio (SNR) with respect to the background is improved.

In Fig. 4 we also compared the proposed method to different approaches proposed by Varon *et al.* [10]. Some of these methods require a manual selection of a reference image. So, in order to have a fair comparison, we selected the reference image that gave the best SNR out of all available for each method. Nevertheless, our automatic method still outperforms all of them.

4. EFFECT OF MODEL SIMPLIFICATIONS IN THE METHANE QUANTIFICATION.

Atmosphere model. We study how different assumptions on the atmospheric model (5) affect the methane quantification with a numerical example. Computations are done without the logarithm to simplify the notations, this however does not change the quantification. We also assume that the sun and viewing angles are zero, *i.e.* $\gamma = 2$ for the numerical applications. For that we suppose that our observation yields a given attenuation

$$\delta R = \frac{u(x,y,t)}{\hat{u}(x,y,t)} = 0.95, \tag{6}$$

we then estimate the concentration from the attenuation using three different models.

For the first model, let us suppose that the atmosphere doesn't absorb any light, *i.e.*

$$\forall f, e^{-2\sum_{i=0}^{l} A_i(f) l_i} = 1. \tag{7}$$

In this case, the observed attenuation δR is

$$\delta R = \frac{u(x,y,t)}{\hat{u}(x,y,t)} = \frac{\int s(f) e^{-2A_{CH4}(f) l_{em}} df}{\int s(f) df}. \tag{8}$$

atmosphere model	estimated excess of CH_4 from $\delta R = 0.95$
no atmosphere	2015ppb
no atmosphere, only 1600ppb of CH_4	2393pbb
realistic atmosphere with 1600ppb of CH_4	2417pbb

Table 1. Estimated excess methane using different atmospheric models with increasing complexity.

For the second model, we consider the atmospheric methane by assuming an atmosphere purely composed of methane and excess methane. The atmosphere consists of l_{atm} cm of methane, which leads to

$$\frac{u(x,y,t)}{\hat{u}(x,y,t)} = \frac{\int s(f) e^{-2A_{CH4}(f)(l_{atm}+l_{em})} df}{\int s(f) e^{-2A_{CH4}(f) l_{atm}} df}. \tag{9}$$

This case can be brought back to the case without atmosphere by considering a second sensibility s' such that $s'(f) = s(f)e^{-2A(f)l_{atm}}$. For the third and last model, we consider a complete, but fixed, atmospheric model as in (5) that also includes atmospheric methane ($l_{atm} = 1.3cm \approx 1600ppb$) generated using [12]. Table 1 summarizes the estimated concentration of methane using the different models. We observe that modeling the atmospheric methane cannot be neglected as it induces a notable bias. On the other hand, the simulation of the rest of the atmospheric gases can be negleted.

Sentinel-2A vs Sentinel-2B. The Sentinel-2 constellation is comprised of two satellites: Sentinel-2A and Sentinel-2B. While they both have very similar sensitivities, they are not perfectly identical. We show here that it is important to take this difference into consideration during the quantification step. For that we consider the same attenuation given in (6). We then estimate the concentration for both configurations of satellites. Using the sensitivity s_A of Sentinel-2A yields an estimated excess of CH_4 of $2393ppb$. Doing the

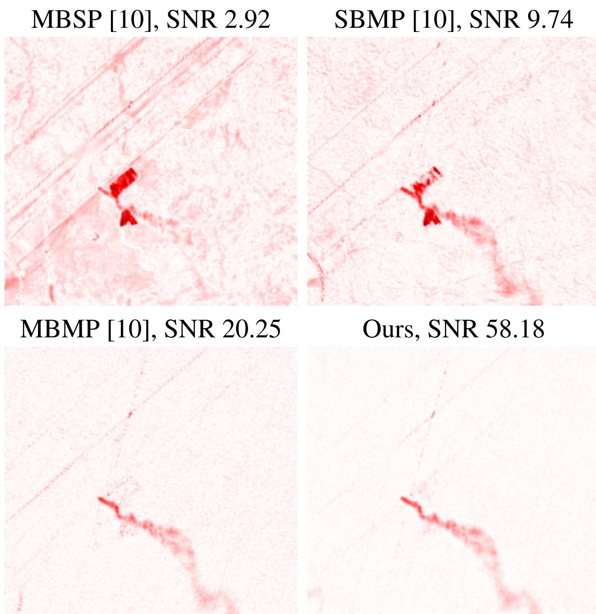

Fig. 4. Comparison between multiple methane excess quantization methods. Our automatic method provides a much better background reconstruction allowing to discriminate and quantify the methane plume better.

same estimation with the sensitivity s_B of Sentinel-2B yields $3194ppb$. This show that it is very important to use the correct sensitivity during the estimation process.

Choosing a fixed methane atmosphere. As mentioned previously, we choose a fixed atmospheric quantity of methane of $l_{atm} = 1.6 \approx 1800ppb$. However, it has been shown that the quantity of methane in the atmosphere is location dependent. We estimated the error due to this approximation by estimating l_{em} for different values of l_{atm}. We saw that for l_{atm} between 1700 and 1900 ppb, the error on l_{em} was at most of the order of $30ppb$. This justify selecting a single fixed value for the quantity of methane in the atmosphere independently from the location.

5. CONCLUSION

We have presented an automatic method for methane quantification using a multispectral satellite like Sentinel-2. Although in this paper we only presented results using Sentinel-2, we have had a similar success using Landsat-8 imagery. The next step is to use controlled releases and a source emission method like IME [13] to measure the total error of our quantification process with an actual ground truth. This will also help us define the precision of the quantification process based on the methane excess emitted from the calibrated source. Having an automatic pipeline paves the way for an automatic detection and quantification pipeline that could provide a global automatic monitoring of the Earth with a short revisit time for methane pollution.

6. REFERENCES

[1] Riley M Duren et al., “California’s methane super-emitters,” *Nature*, vol. 575, no. 7781, pp. 180–184, 2019.

[2] Daniel H Cusworth et al., “Intermittency of large methane emitters in the permian basin,” *Environmental Science & Technology Letters*, 2021.

[3] “Anthropogenic and Natural Radiative Forcing,” in *Climate Change 2013 - The Physical Science Basis*, Intergovernmental Panel on Climate Change, Ed., pp. 659–740. Cambridge University Press, Cambridge, 2013.

[4] David R Lyon et al., “Aerial surveys of elevated hydrocarbon emissions from oil and gas production sites,” *Environmental science & technology*, vol. 50, no. 9, pp. 4877–4886, 2016.

[5] Rebecca Del’Papa Moreira Scafutto et al., “An evaluation of airborne swir imaging spectrometers for ch4 mapping: Implications of band positioning, spectral sampling and noise,” *International Journal of Applied Earth Observation and Geoinformation*, vol. 94, pp. 102233, 2021.

[6] J. Pepijn Veefkind et al., “Tropomi on the esa sentinel-5 precursor: A gmes mission for global observations of the atmospheric composition for climate, air quality and ozone layer applications,” *Remote sensing of environment*, vol. 120, pp. 70–83, 2012.

[7] Sudhanshu Pandey et al., “Satellite observations reveal extreme methane leakage from a natural gas well blowout,” *Proceedings of the National Academy of Sciences*, vol. 116, no. 52, pp. 26376–26381, 2019.

[8] Daniel H Cusworth et al., “Potential of next-generation imaging spectrometers to detect and quantify methane point sources from space,” *Atmospheric Measurement Techniques*, vol. 12, no. 10, pp. 5655–5668, 2019.

[9] Jason McKeever et al., “First methane sensing results from ghgsat’s commercial constellation,” 2021.

[10] Daniel J Varon et al., “High-frequency monitoring of anomalous methane point sources with multispectral sentinel-2 satellite observations,” *Atmospheric Measurement Techniques*, vol. 14, no. 4, pp. 2771–2785, 2021.

[11] Tristan Dagobert et al., “Cloud Detection by Luminance and Inter-band Parallax Analysis for Pushbroom Satellite Imagers,” *Image Processing On Line*, vol. 10, pp. 167–190, 2020.

[12] Steven D Lord, *A new software tool for computing Earth’s atmospheric transmission of near-and far-infrared radiation*, vol. 103957, Ames Research Center, 1992.

[13] Daniel J Varon et al., “Quantifying methane point sources from fine-scale satellite observations of atmospheric methane plumes,” *Atmospheric Measurement Techniques*, vol. 11, no. 10, pp. 5673–5686, 2018.